Fabrication of spintronic material $Cd_{1-x}Mn_xTe$ using stack deposition

P. BANERJEE*, J. PAL, B. GHOSH
*Advanced Materials & Solar Photovoltaic Division, School of Energy Studies,
Jadavpur University, Kolkata - 700 032, India*
E-mail: b_pushan@rediffmail.com

Spintronic materials, employing the spin of carriers as a medium for sending information beside their charges, have drawn significant attention of scientists since the last decade for their uses in multifunctional and energy saving devices. Manganese doped cadmium telluride, $Cd_{1-x}Mn_xTe$, is reported as a material for spin control under the influence of magnetic field due to the presence of manganese.

Stacks of CdTe and MnTe were deposited on basic substrates like glass. After deposition the stacks were given a heat treatment for interdiffusion of materials either to form a solid solution or a composite. The state of the diffusion further indicated about their response in the magnetic field.

In the present study, various numbers of stacks were deposited and annealed at different temperatures to study their response both in electric and magnetic fields. The results thus obtained were fitted in a mathematical model to finalize the optimum condition for fabricating the exact material for spintronic action. The details of fabrication, studies and the responses will be discussed in the text of the paper.
© *2005 Springer Science + Business Media, Inc.*

1. Introduction

The enormous progress achieved today in the field of semiconductor electronics is based on the transport of charge by carriers, namely electrons and holes. One of the ways of achieving this progress has been the rapid miniaturization of electronic devices and circuits. This miniaturization is well described by Moore's law. However, some researchers suggested that today's technology and its development according to Moore's law would last no longer than five to ten years. This inference comes out from a number of technical problems that have to be solved to enhance the performance of the electronic devices further. Some of the problems are of very fundamental in nature viz. the diffraction limit in lithography, grain nature of matter and charge, tunneling of charge through insulators, heat dissipation associated with the switching process of the transistor etc. [1]. In this situation it seems that future electronic devices will have to perform in a multifunctional way by integrating several functions into themselves. Such devices may include processors with memories, sensors with actuators, electronic and photonic devices with magnetic properties etc. Here comes the importance of studying spin dependent phenomenon into semiconductors. In the nanoscale dimension of faster and denser integrated circuits, the spin dependent exchange interactions among carriers can no longer be neglected. To increase the functionalities of the existing devices and circuits like mass storage and processing of information simultaneously and to realize quantum information technologies using spin as a qubit in solid state, the spin degree of freedom has to be exploited.

Spin has numerous advantages over charge: (i) relative immunity to electrical noise, (ii) lower power requirements to manipulate data, and (iii) much longer coherence times in applications such as quantum information processing (computing, cryptography and teleportation) where coherence is a critical issue. It enables spin to find particular importance in quantum computation and communication [2]. Thus, the electronic spin is much more promising than its charge for materialization of the present revolutionary ideas on quantum computation, quantum cryptography, data compression and teleportation.

The semiconductors commonly used for electronic devices and integrated circuits, such as silicon and gallium arsenide, are non-magnetic and so the useful utilization of both charge and spin is unattainable from these materials owing to their small magnetic g-factor [3]. For such materials, the magnetic fields that have to be applied for achieving a useful energy difference between two possible spin orientations, are too high for everyday use. At the same time, the difference in crystal structure between magnetic materials and common semiconductors makes them incompatible with each other. As a remedy to this problem, magnetic elements

---

*Author to whom all correspondence should be addressed.

are introduced into non-magnetic semiconductors to form an alloy called diluted magnetic semiconductors (DMS). Semiconducting spintronic materials, combining charge and spin of carriers to play indispensable roles in realizing functionalities, employ the carrier-induced magnetism in diluted magnetic semiconductors for their operations. Manganese is a common magnetic dopant in such DMS. In II–VI DMS, the magnetic interaction among carriers is dominated by the antiferromagnetic exchange between Mn-spins, resulting in paramagnetic, antiferromagnetic and spin-glass behavior of the materials. II–VI DMS are also found to be ferromagnetic but usually at low temperatures [4].

Spintronic materials can also be used to fabricate solar cells, where one layer of the *p-n* junction is kept as a DMS. Such solar cells generate both charge and spin current. Ordinary solar cells are *p-n* junctions, on which light shines, generating electron-hole pairs and thereby producing electrical currents. A spin solar cell works similarly, but the generated electron-hole pairs have preferred-spin orientation, so the resulting current is both electrical (charge) and spin current [5]. Here, as in ordinary solar cells, light illuminates the depletion layer of a semiconductor (such as gallium arsenide), generating electron-hole pairs. The huge built-in electric field in the layer (typically 10^4 volts/cm) swiftly sweeps electrons into the n region and holes into the p region. If a wire connects the edges of the junction, a current flows. If the light is circularly polarized (from filtered solar photons, for instance), the generated electrons are spin polarized. (Holes in III–V semiconductors—for example, gallium arsenide, indium arsenide and others—which are most useful for opto-spin-electronic purposes, lose their spin very quickly, so that their polarization can be neglected.) As the spin-polarized electrons created in the depletion layer pump the spin into the n region, the resulting current is spin polarized. Hence, photons of light are converted into oriented spins [6]. Such a cell can act as a spin generator for spin devices.

2. Theoretical formulation

Let two individual layers of different materials, labeled "*a*" and "*b*" are stacked along *z*-axis with thickness "*t*" as shown in Fig. 1. The layers are characterized by their intrinsic mean free paths (λ_a, λ_b), relaxation times (τ_a, τ_b) and resistivities (ρ_a, ρ_b). The aggregate resistivity (ρ_{ag}) of the bilayer structure is determined by first calculating the electric field's influence upon the carrier distribution function "*f*" and then calculating the resulting current density in each layer.
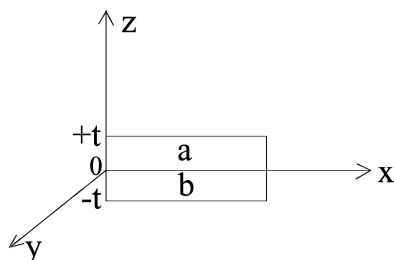

Figure 1 Geometry of bilayer structure.

The local current density in each layer is given by,

$$J(\vec{r}) = 2e \left(\frac{m}{h}\right)^3 \int f(\vec{v}, \vec{r}) \, \vec{v} \, dv_x \, dv_y \, dv_z \quad (1)$$

As such, the distribution function is independent of $x \& y$ and can be written as

$$f = f_0 + f_1(\vec{v}, z) \quad (2)$$

Solving the Boltzmann's transport equation for "*f*" in presence of an electric field, the expression for f_1 comes as

$$f_1(v, z) = \frac{e\tau E}{m} \frac{\partial f_0}{\partial v_x} (1 + g \, e^{-z/\tau v_z}) \quad (3)$$

Applying suitable boundary conditions

$$f_a^+(0) = f_b^+(0); \quad f_a^-(0) = f_b^-(0);$$
$$f_a^+(t) = f_b^+(t); \quad f_a^-(-t) = f_b^-(-t)$$

the values of the coefficient "*g*" for the charges moving in upward and downward direction in the two layers are found out.

Using the values of f_1 and g, the current densities in the two layers are calculated from the Equation 1.

After algebraic manipulations, the aggregate resistivity is calculated as

$$\rho_{ag} = \frac{2\rho_a\rho_b}{\rho_a + \rho_b - 3\lambda_a(\rho_b - \rho_a)(1 - \lambda_b/\lambda_a)F/t} \quad (4)$$

where

$$F = \int_o^{\pi/2} \frac{\cos\theta \, \sin^3\theta \, d\theta}{\coth(t/2\lambda_a \cos\theta)} + \coth(t/2\lambda_b \cos\theta) \quad (5)$$

is a parameter controlling the aggregate resistivity.

For thick film limit, the aggregate resistivity becomes,

$$\rho_{thick}^{ag} = \frac{2\rho_a\rho_b}{\rho_a + \rho_b} \quad (6)$$

Whereas for thin films the expression comes out to be

$$\rho_{thin}^{ag} = \rho_a \frac{(1 + \lambda_b/\lambda_a)}{(\lambda_b/\lambda_a + \rho_a/\rho_b)} \quad (7)$$

In the special case where the conduction electron densities are equivalent in two layers, $\rho_a/\rho_b = \lambda_b/\lambda_a$ and the composite resistivity is given by a simple average

$$\rho_{thin}^{ag} = \frac{\rho_a + \rho_b}{2} \quad (8)$$

3. Experimental methods

For synthesizing the spintronic material $Cd_{1-x}Mn_xTe$, workers in many places around the globe are employing techniques like Bridgman process, molecular beam epitaxy, laser ablation etc. to obtain the material in single crystal form. These processes have some disadvantages like high cost of instrument, low deposition rate etc. In a country like India, some low-cost and less complicated process are to be used so as to give spintronics adequate chance of advancement. The present work utilizes radio frequency sputtering technique to deposit polycrystalline layers of manganese telluride (MnTe) and cadmium telluride (CdTe) onto the substrates followed by heat treatment and other post deposition processing to enhance the film properties.

For some arbitrarily chosen values of the parameter "x", proportionate quantities of MnTe and CdTe thin films were deposited on sodalime glass in the form of stacked layers to form three sets of films. For this purpose, r.f. sputtering unit (model 12″ MSPT of Hind HiVacuum Co.) was used. The details of the deposition parameters are shown in Table I.

After film deposition, a thin (0.05 μm) coating of cadmium chloride was applied over the films using physical vapor deposition. The films were annealed in a furnace at a pressure of about 10^{-2} mbar for 10–40 minutes in temperatures ranging from 100–350°C to promote grain growth. The films then underwent etching process to make the surface tellurium rich by dipping into 5% Br:MeOH solution for 1 second. For each set of temperature, heating time and x-value, the sheet resistivity of the films were determined using four-probe system (model DFP-02, Scientific Equipment Co., Roorkee, India). The actual values of "x" in the films were found out later by energy dispersive X-ray analysis of the samples, which came out to be 0.06, 0.17 and 0.24 respectively.

4. Results

Figs 2 to 4 show the variations in sheet resistivity of the samples with temperature and annealing time for three values of "x". All the figures show that the films responded to temperature and heating time in a similar nature. At lower temperatures, the curves indicate the formation of solid solutions and not compounds. At higher temperatures namely 300 and 350°C, there is a regular rise in sheet resistivity followed by a tendency of saturation, indicating the possibility of reaction between CdTe and MnTe at those temperatures.

The Hall mobility and bulk carrier density of the samples were determined using the standard Vander-Pauw geometry, with silver contact pads deposited at the corners of square films, taking only the films annealed at

TABLE I Deposition parameters for the stack layers

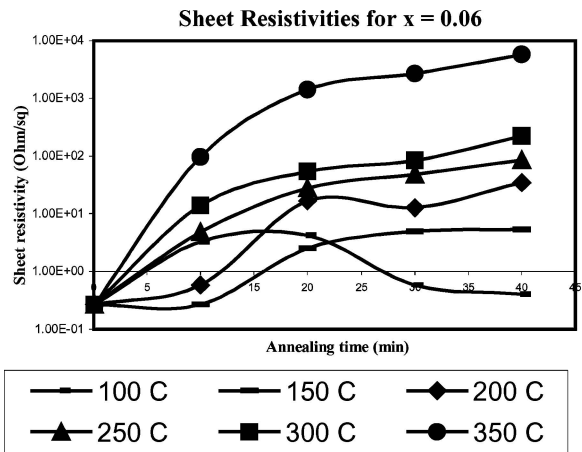| Sputtering target	MnTe & CdTe, 99.99%, 4″ diameter
Plasma gas composition	Argon at 0.02 mbar pressure
Net power density	2.47×10^4 W/cm^2
Total film thickness	1.1–1.3 μm

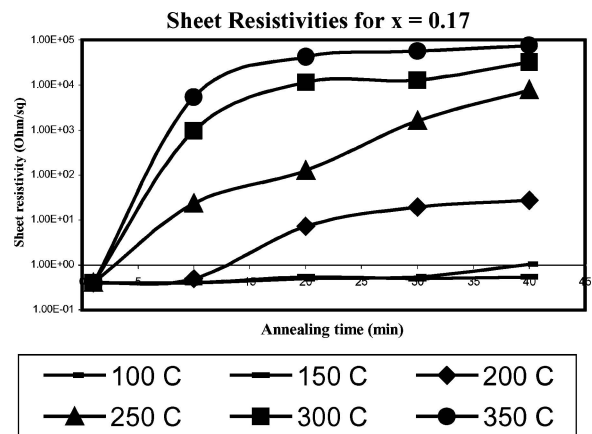Figure 2 Sheet resistivities for $x = 0.06$.
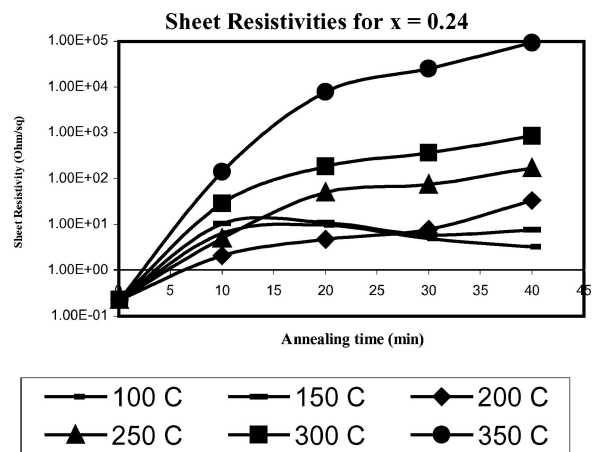

Figure 3 Sheet resistivities for $x = 0.17$.

Figure 4 Sheet resistivities for $x = 0.24$.

300 and 350°C and employing the standard Hall-effect measurement set up (model DHE-21, Scientific Equipment Co., Roorkee, India). The respective values are shown graphically in Figs 5–10.

Figs 5 and 6 show that the nature of change of properties of the samples are opposite at two annealing temperatures (one rising while the other falling)—indicating the formation of a composite structure instead of a regular compound. But from Figs 7 and 8 it is seen that the annealing temperature changes only the values of Hall mobility and Carrier density — the nature
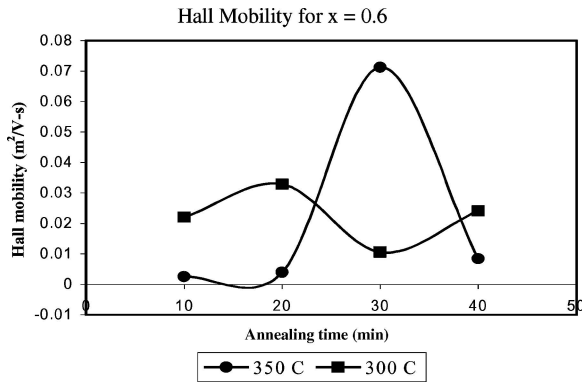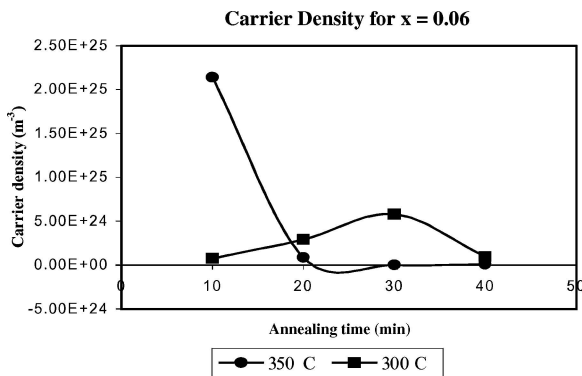
Hall Mobility for x = 0.6

Figure 5 Hall mobilities for $x = 0.06$.

Carrier Density for x = 0.06

Figure 6 Carrier concentrations $x = 0.06$.

Hall Mobility for x = 0.17
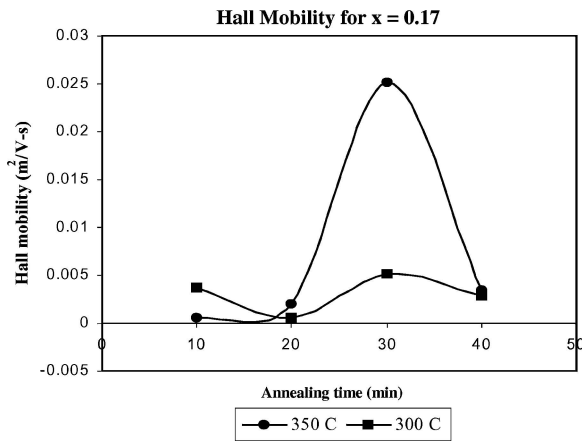
Figure 7 Hall mobilities for $x = 0.17$.

Carrier Density for x = 0.17
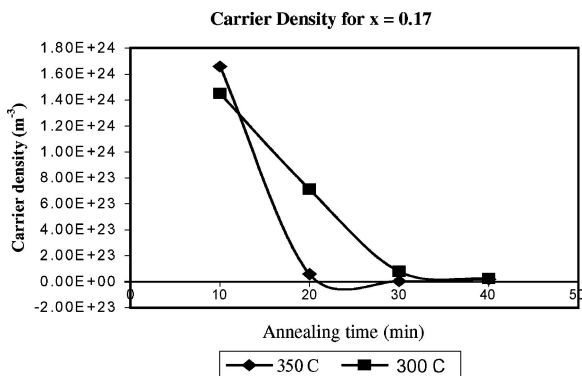
Figure 8 Carrier concentrations $x = 0.17$.

Hall Mobility for x = 0.24

Figure 9 Hall mobilities for $x = 0.24$.

Carrier Density for x = 0.24
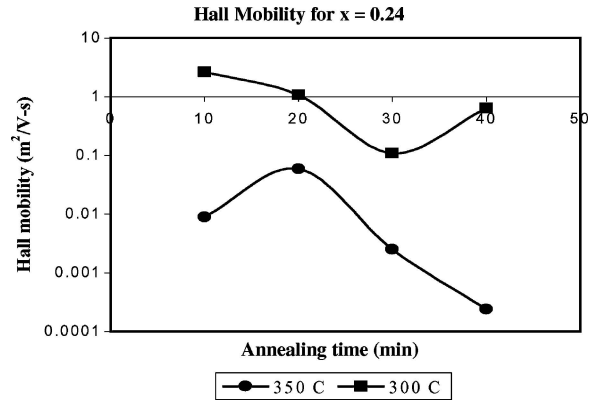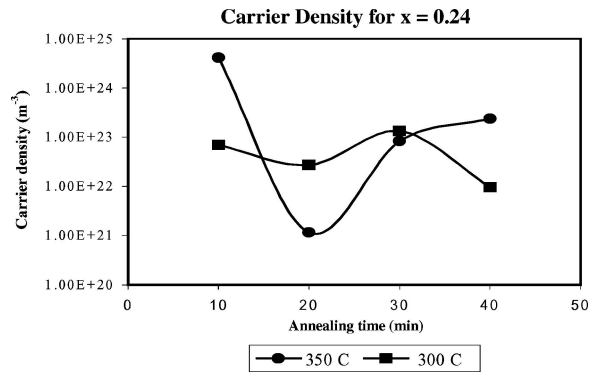
Figure 10 Carrier concentrations $x = 0.24$.

of variation of these parameter with time is alike. This shows that a good bond formation, which is the characteristics of a compound, occurred with that particular value of "x" – 0.17. The Hall mobility maximizes for an annealing time of 30 min and after that, the carrier densities start to be close irrespective of temperature.

The behaviors shown in Figs 9 and 10, on the other hand, indicate the formation of a solid solution between CdTe and MnTe. Films could not be heated further because then its resistivity became too high and ceases the Hall current through it. The characteristic parameters of the best film thus obtained is shown in Table II. Table III shows the individual resistivities of CdTe and MnTe as measured from the sputtering targets and the theoretical values of resistivity calculated from them for thick and thin bilayer-film.

TABLE II Characteristic parameters of the best film

Annealing temperature	350°C
Annealing time	30 min
Hall mobility	2.5×10^{-2} m^2/V-s
Resistivity	6.8×10^{-2} Ω-m
Carrier density	3.6×10^{21} m^{-3}

TABLE III Resistivities as calculated from the theory

Resistivity of CdTe	1.7×10^{-2} Ω-m
Resistivity of MnTe	5.0×10^{-4} Ω-m
ρ_{thick}	9.7×10^{-4} Ω-m
ρ_{thin}	8.7×10^{-3} Ω-m

The resistivity of the bilayer structure as calculated from the proposed theory comes out to be only one order of magnitude lower than the experimental value. This is explainable from the facts that the effect of post deposition treatments of the films enhanced the grain growth and raised the film conductivities. Also, the sputtering targets, from which the resistivities of CdTe (ρ_{CdTe}) and MnTe (ρ_{MnTe}) were measured, have more compact molecular packing compared to the films produced from them. The experimental results thus match with the theoretical predictions.

5. Conclusions

For using a thin film in spin-related applications, Hall mobility plays an important role—better the Hall mobility in a DMS film, better is its response in a magnetic field that is applied to distinguish the two spin states of the carriers. The present study tried to find the condition of forming compound spintronic film $Cd_{1-x}Mn_xTe$ using stack deposition of CdTe and MnTe. From the experimental results it is observed that the optimum time of heating the stack layers is 30 min in the temperature range of $350°C$. The final value of resistivity of the optimized sample matched within reasonable limits with the theory developed for bilayer structure, proving the validity of the theory in a preliminary level. Some other phenomena like diffusion of mass, effect of temperature and annealing time etc. are to be included into the theory to increase its applicability. The other properties of this film like optical band gap, figure of merit, photoresponse, magneto-optic behavior etc. are to be now determined using this optimized condition of fabrication. Another effect to be tested for such spintronic films is the dependence of its properties on the film thickness and number of bilayer, which in the present case is one. Increase in the number of bilayer will enhance the diffusion among layers and improve film properties. Such tasks are kept as the future works on this material.

References

1. T. DIETL, *Acta Phys. Polon. A* **100**(Suppl.) (2001) 139.
2. C. H. BENETT and D. P. DIVINCENZO, *Nature* **404** (2000) 247.
3. H. OHNO, *Science* **281** (1998) 951.
4. A. HAURY, *et al. Phys. Rev. Lett.* **79** (1997) 511.
5. J. FABIAN, in Paper P3.2, MRS Fall Meeting (Boston) 2002.
6. S. DAS SHARMA, *Amer. Sci.* **89** (2001) 516.